1   Hydraulic routing of extreme floods in a large ungauged river and the estimation of associated

2   uncertainties: A case study of the Damodar River, India

3

4   Joy Sanyal, Patrice Carbonneau and Alexander L. Densmore

5   Department of Geography
6   Durham University, Durham, U.K.

7

8   Address:
9   Department of Geography   Email: joy.sanyal@durham.ac.uk
10   Durham University,   Phone: 44 (0) 191 33 41949
11   Science Laboratories   Fax: +44 (0) 191 33 41801
12   South Road, Durham
13   DH1 3LE, U.K.

14

15

16

17

18

19

20

21

22

23

24

25

26

27

28

29

30

31

32

33

34

35

36

37

38

39

40

41

42

43

44

45

Abstract

Many developing countries are very vulnerable to flood risk since they are located in climatic zones characterized by extreme precipitation events, such as cyclones and heavy monsoon rainfall. Adequate flood mitigation requires a routing mechanism that can predict the dynamics of flood waves as they travel from source to flood-prone areas, and thus allow for early warning and adequate flood defenses. A number of cutting edge hydrodynamic models have been developed in industrialized countries that can predict the advance of flood waves efficiently. These models are not readily applicable to flood prediction in developing countries in Asia, Africa and Latin America, however, due to lack of data, particularly terrain and hydrological data. This paper explores the adaptations and adjustments that are essential to employ hydrodynamic models like LISFLOOD-FP to route very high magnitude floods by utilizing freely available Shuttle Radar Topographic Mission (SRTM) digital elevation model (DEM), available topographic maps and sparse network of river gauging stations. A 110 km reach of the lower Damodar River in eastern India was taken as the study area since it suffers from chronic floods caused by water release from upstream dams during intense monsoon storm events. The uncertainty in model outputs, which is likely to increase with coarse data inputs, were quantified in a generalised likelihood uncertainty estimation (GLUE) framework to demonstrate the level of confidence that one can have on such flood routing approaches. Validation results with an extreme flood event of 2009 reveal an encouraging index of agreement of 0.77 with observed records while most of the observed time series records of a 2007 major flood were found to be within 95% upper and lower uncertainty bounds of the modeled outcomes.

Keywords: Hydrodynamic Model, Developing Country, LISFLOOD-FP, SRTM DEM, GLUE, India

1.0. Introduction

The developing world, particularly Asia and Latin America, shares the highest concentration of flood occurrences due to high-magnitude storm events such as tropical cyclones and intense monsoon downpours. According to the EM-DAT database maintained by the Office of US Foreign Disaster Assistance and the Centre for Research on the Epidemiology of Disasters (OFDA/CRED), between 1900 and 2012, 3151 out of 3927 (more than 80 percent) of major floods occurred in Asia, Africa and Latin America. The impact of these disasters is more pronounced in developing economies as the cost of a partial or full recovery in relation to GDP may be very high (Alcantara-Ayala 2002). The technological capability to predict the dynamics of flood waves from upper catchments to low lying flood-prone areas downstream is essential for developing flood warning and flood management strategies, and thus mitigating the effects of these disasters. The last three decades have seen the development of many advanced tools for flood modelling and prediction. However, these technologies are typically not applied in developing countries due to lack of appropriate data. The aim of this study is thus to explore a methodology for utilising advanced flood routing tools in data-sparse settings in the developing world.

Hydrodynamic models have been widely used to route floods with remarkable accuracy. However, they require very high resolution terrain data as well as hydrological inputs from numerous gauging stations. The terrain data that are used for this purpose are typically derived from LiDAR survey, IFSAR such as NEXTMap in the UK at a horizontal resolution of 5 m and vertical accuracy of 0.5 to 1 m (Sanders et al., 2005; Mason et al. 2010) or densely spaced surveyed cross-sections (Pappenberger et al., 2006). Gauging stations are commonly available at the inlet and outlet of the reach being modelled and these stations frequently record water discharge at high temporal resolution (e.g., 15 minute intervals). As an example, Bates et al. (2006) used LiDAR-generated DEMs, in combination with a series of airborne synthetic aperture radar (ASAR) images captured opportunistically during the peak and recession limbs of a flood

hydrograph, in order to calibrate and validate a simple raster-based hydrodynamic model (LISFLOOD-FP). The LiDAR DEM used had <1 m horizontal resolution with a vertical root mean square error of 0.079 m. However, it is well documented that the lack of these data sets for the vast majority of developing countries is a major obstacle for employing hydrodynamic models there (Sanyal and Lu, 2004). In addition, the near-absence of an established network of permanent GPS base stations in many areas means that undertaking ground surveys with differential GPS in order to supplement the paucity of terrain data is also challenging. Hydrologic modelling techniques such as the Muskingum method could be an alternative as they are less dependent on accurate terrain as a model input. Nevertheless, the efficiency of these approaches are not very high due to their inability to account for the hydrodynamic processes associated with extreme floods, particularly backwater and the floodplain storage effects (Garbrecht and Brunner, 1991). The rarity of gauging stations at the downstream end of a flood-prone reach of interest, however, makes even these relatively simple flood routing techniques often unsuitable in large parts of Asia, Africa and Latin America.

India is a good example of this general issue, because it suffers frequently from large scale to localised flooding during the monsoon season and is characterised by a dearth of available data for flood routing that is typical in developing countries in general. During heavy monsoon storms, large dams in India are sometimes forced to release large amounts of water in a short time in order to prevent catastrophic dam breaks, and this release can lead to devastating floods downstream. This situation urgently demands the development of flood routing systems. As limited availability of suitable terrain data is the most significant obstacle for developing a flood routing model in developing nations in general and India in particular, we need to consider the available options carefully. Apart from the freely available Shuttle Radar Topography Mission (SRTM) digital elevation model (DEM) of 3 arc second (approximately 90 m) resolution, the other possible source of terrain data in India are Survey of India (SOI) topographic maps at 1:50,000 scale and 20 m contour interval, and the ASTER Global Digital Elevation Model (GDEM) of 30 m resolution. The large contour intervals and hence the low horizontal resolution and

vertical accuracy of the SOI maps make them unsuitable for hydrodynamic models in flat areas that are coincidentally also the most flood-prone. The ASTER GDEM, although of moderately high horizontal resolution of 30 m, is reported to have a vertical RMSE of 18 to 29 m (Reuter et al. 2009) and is not considered as a suitable terrain input for hydrodynamic modelling. In contrast, Sanders (2007) compared the performance of the SRTM DEM with a very accurate LiDAR DEM for hydrodynamic modelling, and pointed out the worth of the SRTM DEM as a global source of terrain data. Paiva et al. (2011) employed some generic rules of fluvial geomorphology in a GIS-based algorithm to derive simplified channel geometries from the SRTM DEM for 1D hydrodynamic modelling of a major tributary of the Amazon River. Modified SRTM DEMs have also been employed with the MIKE21 2D hydrodynamic model for simulating the seasonal dynamics of the Nile swamps of in southern Sudan (Petersen and Fohrer 2010). However, undertaking a fully 2D hydrodynamic modelling for a reach length of more than 100 km is likely to be associated with quite high computational cost.

Other studies have used river cross-sections derived from the SRTM DEM in order to route river flow in the Mahanadi River delta (Patro et al. 2009a; Patro et al. 2009b) and the Brahmani River basin (Pramanik et al. 2010) in India with the MIKE11 1D hydrodynamic model. Although these studies have showed that the SRTM DEM or its modified forms can be used to extract cross-sections for large-scale 1D flow routing, such an approach may not perform equally well where the accuracy of the DEM, especially over the river channel, is not consistent. The accuracy of flood routing can be very sensitive to DEM accuracies in the channel when dealing with extreme events (Casas et al., 2006). Some of the afore-mentioned studies such as Patro et al. (2009) had access to significant secondary information, like surveyed embankment heights, which may not be available in all flood-prone reaches. More broadly, employing sparse data inherently increases the uncertainties of the model predictions, but studies in the literature have rarely reported formal uncertainty analysis of model outputs that are derived from coarse terrain and hydrological inputs. A notable exception to this was the study reported by Pappenberger et al. (2006) that dealt with the influence of uncertain boundary conditions on HEC-RAS model output. To

address this gap, the main objectives of this paper are 1) to find a suitable technique to route high magnitude and low frequency floods with the SRTM DEM, making use of limited cross-section surveys and no gauging record at the outlet and 2) to assess the uncertainty in model outputs that are induced by poor quality hydrologic and terrain inputs.

2.0.   Study Area

The Damodar River Basin, with an area of 24,235 km^2, spreads across the Indian states of Jharkhand and West Bengal. The source of the river lies in the dissected Chotanagpur Plateau at a height of approximately 610 m above mean sea level. The river flows for 540 km, initially eastwards before turning southwards to join the Hoogly River (one of the main distributaries of the Ganges). As the river is heavily silted, the lower valley does not have the capacity to cope with a peak discharge of more than 2300 m^3/s (Central Technical Power Board India 1948). The lower Damodar Basin suffers from chronic flooding. There were 16 major floods recorded between 1823 to 1943, with a peak discharge of 18,500 m^3/s recorded at Durgapur in 1913 and 1935 (Saha 1979). The devastating flood of 1943 led to the establishment of the Damodar Valley Corporation, a multipurpose river valley project that built a network of dams to moderate flood waves and provide irrigation during the dry post-monsoon season. Although building the dams arguably achieved its objective of moderating flood waves, the lower Damodar Basin was still subject to flooding 14 times in the post-dam era of 1958 to 2000 (Chandra 2003). More recently, this area witnessed major floods in the year 2006, 2007, 2009 and 2011. The study area for the present investigation extends from the Durgapur Barrage to the point where the main channel bifurcates into two distributaries (Fig. 1). The length of the study reach is approximately 110 km with an average width of 1.5 km.

The flow of water during high magnitude floods in our study reach is primarily confined within the bankfull level, with occasional overtopping of the levees on the right bank. The floodplain flow,

whenever it takes place, is intermittent in nature. There are some reasons for selecting this reach for the present study. Firstly, predicting the travel time of flood waves from Durgapur Barrage to the downstream end of this reach and forecasting the river stage at this point is of primary interest because the areas situated further downstream of our study reach in West Bengal experience widespread floodplain flow. Also, Durgapur Barrage is the most downstream dam on the Damodar River and the flooding in the lower Damodar Basin is the direct result of the water release from this dam. Thirdly, there is no major structure downstream of the Durgapur Barrage that may affect the natural flow of water. Lastly, regular availability of discharge records at 1 to 3 hour intervals from the barrage and records of river stages at the Jamalpur gauging station at an intermediate location in the study reach (Figure 1) made it possible to procure the necessary hydrological input, calibration and validation data.

3.0.   Data used

Version 4 of the SRTM DEM (90 m horizontal resolution) was downloaded from http://srtm.csi.cgiar.org/. This version of the SRTM DEM is the most reliable and has been supplemented with auxiliary DEMs to fill the data voids. The vertical accuracy of this dataset was reported to be 7.58 m for Phuket Island of Thailand and 4.7 m in the Catskills Mountains in the USA (Gorokhovich and Voustianiouk 2006), while global validation studies of the SRTM DEM have reported an absolute vertical error of 6.2 m for Eurasia (Farr et al, 2007). Hofton et al. (2006) observed that the presence of large plots of dense canopy exaggerates the SRTM DEM elevation. As the floodplain and the river banks of our study reach have frequent clusters of trees and rural hamlets, a positive error in the SRTM DEM can be expected, and the methodology section addresses this issue by correcting the obvious inaccuracies in our terrain data. Apart from the DEMs, spot heights from the Survey of India (SOI) topographic maps were also collected as a source of elevation data in order to estimate errors of the SRTM DEMs in our study area. The maps were mostly at 1:50,000 scale with a few at 1:25,000 scale. A spheroid

transformation was done in order to project the SOI maps from the Modified Everest to WGS84 spheroids so that the maps and SRTM DEM remain in the same coordinate system. There is also a potential degree of nonconformity between the SRTM DEM and the SOI spot heights due to the difference in the vertical datum used by these two datasets. SOI spot heights are elevation from local mean sea levels while SRTM DEM uses the EGM96 geoid model (Lemoine et al, 1996) as the vertical datum (Jarvis et al. 2008). A number of ad-hoc measurements were taken across our study area at known SOI spot height measurement sites with a differential GPS, and the difference was never found to be more than 50 cm. Since the SRTM DEM has a precision of 1 m we decided that SOI spot height and SRTM DEM pixel values are comparable.

The discharge records from the Durgapur Barrage were used at the inlet of the modelled river reach. Specifically, discharge records at 3 hour intervals for a flood event on 25-30 September 2007 and at 1 hour intervals for an event on 7-13 September 2009 were used as model inputs (Fig. 2). In addition, a time series of annual maximum discharge from 1978 to 2010 was also obtained to compute the return periods/exceedance probability of the 2007 and 2009 events, assuming a log Pearson Type III distribution (Fig 3). The hydrographs of the 2007 event, with an exceedance probability of 0.11, and the 2009 event, with an exceedance probability of 0.05, were used as the calibration and validation data. Here, a flood with an exceedance probability of 0.05 means that at any given year there is 5 percent chance of experiencing a flood of 2009 magnitude or more. These floods, with peak discharge values having a return period of approximately 10 years or more, were selected for this study because we are not aware of any previous attempts at estimating hydraulic routing of such damaging events with the SRTM DEM as the only available terrain input. The 2007 and 2009 events were also preferred for this study against other high magnitude events, such as 1978 and 1995, as they occurred quite recently in relation to the time of our field survey which was conducted in 2010. Water levels measured at 1 hour intervals at the Jamalpur gauging station (located approximately 100 km downstream of Durgapur Barrage) were used for the purpose of calibration, validation and uncertainty estimation of the modelled stages for both the 2007 and

2009 flood events. These stage data were only available for high flow period during the floods, and the model performance was measured only against those data. There was no gauging station at the downstream end of the study reach, which is located 20 km downstream of Jamalpur station. All hydrological records were obtained from the Irrigation and Waterways Department of West Bengal, India.

4.0.   Methods

4.1.   Cross-section Surveys

Due to limited resources, we were able to survey only 9 cross-sections, shown with numbers in Fig. 1, along the 110 km study reach. Cross-sections were surveyed at the inlet and outlet of the reach and at the Jamalpur gauging station. The rest of the 6 cross-sections were surveyed at places that represent the typical channel conditions regarding the width, depth, and bed material in that part of the study reach. Easy road access to the river bank was also an important factor that influenced the selection of survey sites. The Damodar River is fed by rainwater and during the dry post-monsoon season only about 10 percent of the channel width is generally occupied by the flowing water. Here we define channel width by the bankfull width normally filled with water during the peak of the monsoon season. The left bank of the study reach has a continuous artificial embankment which is more than 5 m higher than the river bank and very rarely breached during floods. Occasionally there are natural levees and short local artificial embankments on the right bank of the river.

The fieldwork was conducted during November-December, 2010, using a combination of differential GPS (dGPS) to survey the dry river bed and the water surface elevations, and a hand-held portable depth sounder to measure depths below the water surface. Special care was taken to measure the elevation of the water surface at the time of surveying (Fig 4). The measured depths were then subtracted from the water

1   surface elevation to obtain the bottom elevation of the wet part of the channel. As the water level is

2   expected to be at approximately same elevation at the two banks of the wet channel it gave us a very

3   useful indirect measure of the relative accuracy of the DGPS survey.

4

5   The presence of a GPS base station within 20 km of the rover location is an essential prerequisite for

6   conducting any dGPS survey with relatively inexpensive single frequency (L1) GPS receivers. No real-

7   time observations of permanent GPS stations are available in the public domain in India, and the nearest

8   International GNSS Service (IGS) base station was more than 2000 km from our study area. A base

9   station with known coordinates in the International Terrestrial Reference Frame (ITRF)/WGS84 was

10   essential for this survey in order to make the observations consistent with the global datasets such as the

11   SRTM DEM. Many web-based free services can, however, correct a sufficiently long observation (more

12   than 4 hours) of a dual frequency (L1 and L2) GPS receiver from decimetre to centimetre accuracy. A

13   comprehensive review of these services can be found in Tsakiri (2008). We used the Natural Resources

14   Canada's Precise Point Positioning (PPP) service, also known as CSRS-PPP, which uses very precise

15   GPS orbit or clock estimates from IGS to correct user-supplied observations. CSRS-PPP has reported that

16   only 2 hours of continuous observation in dual frequency receivers are capable of achieving a vertical

17   accuracy of approximately 4 cm and with more than 2 days of continuous observation it can achieve a

18   vertical error of 11.8 mm (Ebner and Featherstone 2008). Other services that use the nearest available IGS

19   base station data to apply a differential correction to the user-supplied observation were not used, because

20   differential corrections that are based on distant (e.g. more than 300 km) IGS stations are likely to be of

21   lower positioning accuracy (El-Mowafy 2011).

22

23   At each survey site, a ~4 hour dual frequency GPS observation provided the base station observation, as

24   this duration was sufficient to achieve 5-8 cm errors for the base station position. After the survey, the

25   GPS data were converted into Receiver Independent EXchange (RINEX) format and uploaded to the

26   CSRS-PPP service. A single frequency PROMARK3 GPS was used as the rover for collecting points

1   over the channel. We took static observations at two points by occupying the points for more than 20

2   minutes. These two points are depicted as point A and B in Fig. 4. The actual survey was done in a rapid-

3   static mode. The rover was initialised by occupying point A for 30 seconds and thereafter each surveyed

4   point was occupied for 30 seconds. Special care was taken not to lose the satellite lock once the rover was

5   initialised over a known point (here point A). After the survey was completed an additional observation

6   was taken at point B without losing the satellite lock which was used as the measure of accuracy for the

7   rapid-static survey. It was assumed that static points are likely to have higher accuracy than the rapid-

8   static points and therefore can be used as the reference for measuring the accuracy of the rapid-static

9   measurements. The rover data were post-processed in the Thales GNSS Solution software as described

10   below:

11   i)   The CSRS-PPP output was used as the known coordinates for the base station. The Z coordinate,

12   supplied in ITRF/WGS84 ellipsoid height, was converted into orthometric height using the EGM96 geoid

13   model   available   freely   for   download   from

14   http://cddis.nasa.gov/926/egm96/new_improved.html#geoidgrid. The orthometric height (OH) was

15   calculated as OH = WGS84 Ellipsoid Height - EGM96 Height

16   ii)   The L1 observations of the static points, A and B were differentially corrected with reference to

17   the base station established in step i.

18   iii)   The corrected coordinates of point A were used as a known point and the rapid-static

19   observations were corrected with the base station observation to get the final cross-section data with the

20   planimetric coordinates in latitudes and longitudes and elevation as orthometric heights.

21

22

23

24

25

26

4.2. *Error analysis and modification of the STRM DEM*

2

3 A total of 218 spot heights were obtained from SOI topographical maps and were compared with the

4 corresponding pixel values of the SRTM DEM. Fig. 5a depicts the location of SOI spot heights and shows

5 a bias in their concentration towards the upstream portion of our study area. This was primarily because

6 of the availability of more detailed topographic maps at 1:25,000 scale in that area. There is no systematic

7 correlation between elevation values from the SRTM and SOI maps (Fig. 5b, 5c), indicating that there is

8 no relationship between error and increasing elevation, in contrast to the results of Pramanik et al. (2010)

9 in an area approximately 350 km southwest of our study area. A histogram of differences between the

10 spot heights and the SRTM DEM (Fig. 5d) shows that 28.4 percent of errors lie within a value of ± 2 m

11 (that is, the SRTM DEM is 2 m higher than the observed SOI spot heights).

12 Because of the lack of trends in the distribution of error, the SOI median error value (2 m) was subtracted

13 from the entire SRTM DEM dataset of our study area. Also, in order to reduce local spikes in elevation

14 caused by the presence of trees or settlements, we manually digitised all such features in the floodplain

15 from GoogleEarth. Those polygons were imported in the ERDAS Imagine software and the SRTM DEM

16 was modified by replacing the pixels under the polygons with a smooth surface created by fitting a spline

17 interpolated plane with the pixel values located at the edge of the polygons. To evaluate the effect of these

18 modifications, we compared the modified SRTM DEM with the independent GPS data collected from the

19 channel. The modifications produced a substantial increase in accuracy for the SRTM DEM when

20 compared with the GPS data (see Table 1).

21

22

23

No. of Observation	Mean	Median	Mode
218 (SOI)	-2.13	-2	-2
210 (GPS)	-3.26	-3.17	-3.86
After modification of the raw SRTM DEM			
210 (GPS)	-1.47	-1.2	-0.5
RMSE calculated with 260 SOI spot heights = 2.05			

1 **Table 1** Computed central tendency figures of the SRTM DEM error before and after the modification.
2 All figures are in metres. –ve figures signify that the SRTM DEM cell values are higher than the known
3 elevation values of the same location. GPS surveyed points for the channel recorded a decline in error
4 from -3.17 to -1.2 m after the median error derived with respect to the SOI spot heights was subtracted
5 from the SRTM DEM.

6

7 Finally, we noted that the left river embankment was not clearly visible in its correct alignment in the

8 original SRTM data, probably because its width is less than the pixel dimension (< 90 m) of the DEM.

9 Therefore we created an artificial 15 m high embankment on the modified SRTM DEM, following the

10 actual alignment of the left embankment, in order to prevent the modelled flood water from extending

11 beyond   the   left   embankment.

12

13   *4.3.   Hydrodynamic Modelling*

14

15 Encouraged by the success of previous studies such as Patro et al. (2009a) and Pramanik et al. (2010) in

16 routing flows with SRTM DEM-based cross-sections, we set up a similar 1D hydrodynamic simulation

17 using the HEC-RAS model. However, preliminary experiments gave unstable results at peak flow and it

18 was therefore decided that a simpler modelling framework would be used. 2D hydrodynamic models are

19 more robust in their treatment of flood waves, particularly for the floodplain component of the flow. As a

13

1   full 2D model for a 110 km river reach involves a high computational cost, we used the simple

2   LISFLOOD-FP model (Bates and De Roo 2000). LISFLOOD-FP combines the virtues of both 1D and 2D

3   approaches, where an implicit Newton-Raphson scheme is used for kinematic approximation to the full

4   1D St Venant's equation for channel flow and a raster-based storage cell approach is used in order to give

5   an approximation to a 2D diffusive wave for floodplain flow. The current version also includes a diffusive

6   wave formulation of 1D channel flow. Although LISFLOOD-FP has been successfully used in various

7   small to medium size rivers, mainly in Europe where the required terrain input is available at very high

8   spatial resolution and hydrologic input at very high temporal resolution (Horrit and Bates, 2001; Horrit

9   and Bates, 2002; Bates et al., 2010; Neal et al., 2011), its application to wide rivers such as the Damodar

10   has been limited. One such study was conducted by Wilson et al. (2007), who aggregated the SRTM

11   DEM to 270 m resolution to reduce the overall error and increase the precision of the data and fed these

12   data into LISFLOOD-FP in order to analyse the seasonal flooding pattern of the Amazon River. Although

13   this study did not focus on routing discrete high magnitude flood events, they reported a 0.99 m RMSE in

14   river stages at high water.

15   The primary preference for selecting LISFLOOD-FP came from its simple requirements of terrain input,

16   particularly for the channel. In LISFLOOD-FP the channel is represented by a series of points, each

17   having one value for the bed elevation and another for the channel width. The channel is assumed to be

18   rectangular for computational efficiency. Since we need a single value for the bed elevation at each point

19   of the 1D channel vector instead of a series of points captured by the cross-sections the water surface

20   elevation was used to obtain it. Fig. 6 and 7 show that, at very low flow when the survey was conducted,

21   the elevation of the water level is a very good approximation of the channel bottom of a roughly

22   rectangular channel. The water surface elevation at the cross-sections, when connected along the

23   longitudinal profile of the river, also provides a good approximation of the energy gradient of the river

24   which is important information for any hydrodynamic model.

1   The bankfull channel width was estimated from high resolution images in GoogleEarth and the bed

2   elevation was derived at each point by linearly interpolating between the surveyed elevations of the water

3   surface along the longitudinal profile of the river (Fig. 8a). As the channel component in the LISFLOOD-

4   FP model is unable to handle a flow split or channel bifurcation in the 1D framework, routing the flood

5   became less efficient near the river islands that are occasionally present in our study reach. Only the

6   primary channel as identified from GoogleEarth was represented in 1D, and the secondary channels

7   around islands were simply considered as part of the floodplain and handled by the 2D storage cell

8   framework (Figure 9). The study reach was represented with 129 points which were carefully chosen to

9   represent the varying width of the channel. There was no gauging station available at the downstream

10   boundary of the study reach, and hence there were no data for imposing a water level at the model outlet.

11   In order to minimise the effect of an uncertain downstream boundary condition, we artificially extended

12   the channel vector for few hundred metres with an artificially steep slope. Our intention was to create an

13   artificial torrent at the downstream boundary and to use a fixed water surface elevation corresponding to

14   very low flow as the downstream boundary condition for the model. The Manning's roughness coefficient

15   (n) of the channel was taken as the calibration parameter. As the entire study reach is characterised by a

16   relatively uniform sand based channel bed, a global n value for the channel was used for the calibration

17   runs. Initial estimates for the channel n values were taken from Chow (1959). It is well known that

18   LISFLOOD-FP is less sensitive to the floodplain roughness coefficient and this was kept at 0.035 which

19   is the normal value for farmlands given by Chow (1959).

20

21   A high magnitude flood event of September, 2007 was used to calibrate the model and validation was

22   performed with the extreme event of September, 2009. The diffusive wave formulation for the 1D

23   channel component was used, as Trigg et al (2009) reported that this method is suitable for subcritical

24   flow for channels with shallow bed slope and is able to capture downstream propagation of flood waves

25   along with the response of flow to free surface slope. The model performance was measured using hourly

1   river stage data at the Jamalpur gauging station. Various efficiency criteria have been used in hydrology

2   to quantify how accurately observed records are reproduced by numerical simulations. These measures

3   include but are not limited to the Nash-Sutcliffe efficiency (E), the coefficient of determination (r^2), and

4   the index of agreement (d). In this study, the index of agreement (d) proposed by Wilmot (1984) was used

5   for judging the efficiency of the LISFLOOD-FP model. Here, d is defined as

6

7    $$d = 1 - \frac{\sum_1^n (O_i - P_i)^2}{\sum_1^n (|P_i - \bar{O}| + |O_i - \bar{O}|)^2}$$ (1)

8

9   where O_i and P_i are observed and modelled data respectively, $\bar{O}$ is the mean of the observed series, n is the

10   number of observations in the time series and i is the number of data points. Legates and McCabe (1999)

11   argued that d is a better performance measure than E and r^2 because it is more sensitive to the differences

12   in the modelled and observed means and variances.

13

14

15   *4.4.   Quantifying uncertainty*

16

17   Use of sparse data inputs inevitably increases the degree of uncertainties in the model output. When we

18   are dealing with a disaster warning model, a quantitative estimate of the uncertainty is an essential

19   prerequisite for this kind of system before they qualify for the forecasting of a severe natural hazard. In

20   this paper, the uncertainty of our model predictions was quantified in generalised likelihood uncertainty

21   estimation (GLUE) framework as proposed by Beven and Binley (1992). Uncertainty estimation of

22   LISFLOOD-FP within a GLUE framework has been previously carried out by using synthetic aperture

23   radar images of the extent of flooding as the observed data (Aronica et al. 2002; Hall et al. 2005; Stephens

1   et al. 2012). However, utilising observed stage records for analysing uncertainty of LISFLOOD-FP

2   output is relatively rare (see Hunter et al. 2005 for an exception).

3   In the GLUE framework, a set of behavioural models, that is, a set of inputs and model parameters that

4   reasonably replicate an observed phenomenon, are weighted according to a likelihood measure. The

5   likelihood measure is commonly an objective function that reflects the performance of each set of models

6   during calibration (Beven 2010). Beven (2001) pointed out that a number of decisions, some of which are

7   subjective, have to be made for implementing the GLUE methodology in order to obtain an uncertainty

8   estimation for a hydrological model. These decisions include the range of uncertain parameters, a

9   sampling method for drawing the parameters from the chosen range, an appropriate likelihood measure,

10   and classification of a model as non-behavioural based on the chosen measure. We identified four types

11   of uncertain inputs in our study: 1) the Manning's roughness coefficient (n) for the channel, 2) the fixed

12   water level at the downstream boundary of the model, 3) the channel width and 4) error in the modified

13   SRTM DEM. In the absence of any information to the contrary, we assumed that the uncertainty is

14   uniformly distributed for all four input types. The values of n were decided from preliminary calibration

15   of the 2007 flood event with observed river stages at Jamalpur gauging station, and were set to be from

16   0.020 to 0.030. The range of the somewhat arbitrary fixed water level at the downstream boundary was

17   chosen to be between 12.25 to 14 m. The low end of this range was set to be just greater than the bed

18   elevation of the last point of the river vector, 12.20 m, to ensure that at the initial state the entire study

19   reach remained wet. This measure provided some degree of stability to the model in the initial spin-up

20   period. The high end estimate of 14 m was chosen because this is the water surface elevation during very

21   low flow conditions, as were sampled in our survey. Any higher value of fixed water surface elevation at

22   the outlet would function as a wall and artificially impede efficient drainage of water from the model

23   domain. Channel width was derived from high resolution Geoeye-1 imagery (1 m spatial resolution)

24   available in GoogleEarth. At the majority of points along the channel vector, the river bank was clearly

25   distinguishable from the channel by the permanent vegetation line and it was decided that the maximum

1   possible error in measuring the channel width would not be more than ± 20 m. However, we identified 8

2   points in the channel vector where clear demarcation of the river banks were difficult due to the absence

3   of a clear vegetation line, evidence of channel shifting, or agricultural practice on the channel bed. After

4   careful consideration the channel width at each of these points was allowed to vary in a random fashion.

5   The amount of this variation depended on the degree of uncertainty present in the measurement of

6   bankfull width from GoogleEarth at each of the 8 identified locations and ranges from ± 80 m to ±150 m.

7   Finally, the range of error for the modified SRTM DEM was determined from a semivariogram model of

8   error distribution (Fig 10). The error was computed by subtracting the SOI spot heights from the modified

9   SRTM DEM. Some of the SOI spot heights that were located at the periphery of the model domain or

10   over very high ground, not likely to be inundated in any flood event, were omitted from the semivariance

11   calculation. A lag of 1000 m, which was very close to the average nearest neighbour distance, and a total

12   of 30 lags were used. The range of the semivariogram of error (Fig 10) revealed that the error is spatially

13   autocorrelated for a distance of ~ 3000 m. An unconditional Gaussian Sequential Simulation (GSS) was

14   performed with the derived semivariogram of error using the Geostatistical Analyst extension of ArcGIS

15   10.0 to produce 3000 realisations of error surfaces for the entire model domain. These error surfaces were

16   added with the modified SRTM DEM to produce the input for the uncertainty analysis. Comparison

17   between semivariograms for the DEM before (Fig 11a) and after the addition of error surface (Fig11b) did

18   not revealed any significant change in the spatial autocorrelation pattern of the elevation values. However,

19   for similar lag values the DEM with added error component showed a slight increase in the semivariance

20   values compared to the modified SRTM DEM.

21   The index of agreement (d) was selected as the objective function for computing the likelihood weights.

22   This measure ranges from 0 to 1 and increases monotonically with better model performance, and hence

23   is appropriate for use as a likelihood measure in the GLUE environment.

24   The GLUE methodology was implemented in the following steps:

1   1) The LISFLOOD-FP model was run 3000 times with randomly chosen values for n, river stage at the

2   model outlet and variation in the terrain as described above, following a Monte Carlo approach.

3   2) The values of d were computed for all model runs by comparing the modelled stage output at the

4   Jamalpur gauging station with the observed record. After consulting the model sensitivity graph (Fig 12)

5   a d value of 0.75 was used as the cut-off to distinguish between behavioural and non-behavioural models.

6   According to this criterion 1918 out of 3000 runs qualified as behavioural models.

7   3) The d values were rescaled using the following formula so that the models with higher performance are

8   assigned very high likelihood weight:

9                            $L_i = d_i - Min(d) / Max(d) - Min(d)$ (3)

10

11   where L_i is the likelihood measure of realization i, d_i is the d value for realization i and Max (d) and Min

12   (d) are the maximum and minimum value of the computed index of agreement for the 1918 behavioural

13   model runs.

14   4) Each of these L_i values was divided by the sum of all 1918 computed L values so that the series adds

15   up to 1. The resulting series constituted the final likelihood weights.

16   5) For each time step, the modelled stage values at the Jamalpur gauging station were put together with

17   their final likelihood weights and sorted in ascending order according to the simulated stage values. Then,

18   the cumulative sum of the likelihood weights was computed and upper and lower 95 % uncertainty

19   bounds were obtained by deriving the stages that corresponds to the 5th and 95th percentiles of the

20   cumulative likelihoods. This process was repeated for each 1-hour time step for which the observed data

21   was available. The entire process was automated using MATLAB. We used the readstage.m code

22   (Wilson, 2012) in order to read the stage outputs of the LISFLOOD-FP model.

23

5.0.   Results

5.1.   *Flood routing*

We took the channel Manning's n as the calibration parameter. Fig. 12 shows how the model performance steadily declined with increasing values of n. The model performed best at a relatively low n value of 0.022. The best calibrated result for the 2007 flood event, with a channel n value of 0.022 and an index of agreement (d) of 0.79, is shown in Fig. 13. The September 2009 flood event was then simulated in a similar model setup using the calibrated channel n value of 0.022, yielding a d value of 0.77 (Fig. 14) .

Variability of the discharge at the model downstream boundary for the 3000 MonteCarlo simulations is shown against the figures from the best calibrated output for the 2007 event in Fig. 15. There is some attenuation in the flood hydrograph over the 110 km study reach (see Fig 2a). We did not have any measured discharge data at the model downstream boundary. Assuming a similar pattern of difference between the modelled and observed records as found in the case of river stage at Jamalpur gauge (Fig 13), situated ~20 km upstream of the model downstream boundary, we realise that the best calibrated simulation of the outflow discharge at the model downstream boundary is likely to underestimate the actual discharge consistently. Level of this underestimation is expected to be more pronounced during the rising limb of the flood while during the descending limb the simulated figures possibly lie just below the actual ones. The 3rd quartile of all simulated flow figures at each time step was found to be very close to the rising limb of the best calibrated hydrograph. It indicates that during the rising limb of the hydrograph majority of the simulation runs could not produce a pattern of outflow discharge that is even close to the best calibrated level which is likely to be quite lower than the actual. However, we find that the descending limb of the best calibrated outflow discharge curve lies slightly below the median of the simulated figures at each time step. It illustrates that a substantial portion of the MonteCarlo simulations performed comparatively well after the flood peak was attained.

1   *5.2.   Uncertainty estimates*

2

3   The dotty plots in Fig. 16 are scatter diagrams of each of the uncertain model inputs against their

4   corresponding d values. For each individual parameter dimension the dotty plot represents a projection of

5   sample points onto the goodness of fit response surface (Beven, 2001). Each dot represents an output of

6   one of the Monte Carlo model runs. Fig 16a shows that the model was very sensitive to the channel

7   roughness coefficient, but the variation in fixed water level at the downstream boundary has very little

8   effect on the model performance (Fig 16b). Similarly, variations in channel width had no significant

9   influence on model performance, even for sites at which the exact channel width was quite uncertain (Fig

10   16c). Similar plots constructed at various other points where the channel width was allowed to vary for >8

11   0m showed comparable results and are not included here. We would also like to point out that the indices

12   of agreement of the highest performing models are higher than what was achieved during the calibration

13   stage. The uncertainty plot of the modelled river stages at the Jamalpur gauging station (Fig. 17) reveals

14   that a substantial portion of the observed flood stages are within 95% lower and upper uncertainty bounds

15   for the 2007 event. However, Fig. 17 also illustrates the inability of LISFLOOD-FP to accurately predict

16   the rising limb of the flood hydrograph, and there is consistent underestimation of the water level.

17   6.0.   Discussion

18

19   *6.1.   The terrain data*

20

21   The SRTM DEM for the channel in our study area is characterised by extensive stretches of flat terrain

22   and steps along the longitudinal profile of the river (Fig. 8). In order to find out the cause of this problem,

23   the Version 4 SRTM DEM, used in our study, was compared with the 'Unfilled Finished A' version of the

1   data (downloaded from Global Land Cover Facility Website: http://glcf.umiacs.umd.edu), especially for

2   the channel of the Damodar River. It was found that the two datasets are almost identical except for the

3   existence of a very few isolated bad data pixels in the 'Unfilled Finished A' product which were probably

4   replaced by interpolation from neighbouring pixels in Version 4. This finding confirmed that no

5   supplementary DEM such as ASTER GDEM was used for the channel portion in the Version 4 of the

6   SRTM DEM, because no such data were used in the creation of 'Unfilled Finished A' product. However,

7   when the Version 4 product was compared with the 'Unfinished A' product we found that the unfinished

8   product did not have the same flat surfaces over the channel, but instead the channel was characterised by

9   a unrealistic noisy surface. The unfinished product thus provides a worse representation of the channel

10   long and cross-profiles as compared to Version 4 of the data. The flat surfaces in the 'Unfilled Finished A'

11   and subsequently in the Version 4 products were probably created during the generation of the 'Unfilled

12   Finished A' product as Slater et al. (2006) pointed out that one of the finishing requirements for this

13   product was to monotonically step down the elevation of rivers with more than 183 m width.

14   After lowering the SRTM DEM by 2 m to reduce the error we found that there was considerable

15   mismatch between the bed slopes of the longitudinal profile derived from the SRTM DEM and those

16   obtained by the ground survey (Fig. 8a). These factors likely contributed to the failure of our preliminary

17   attempt with HEC-RAS that was based on cross-sections derived from the SRTM DEM. Unlike Patro et

18   al. (2009a) we did not have access to surveyed embankment heights, because no such comprehensive

19   record exists for the lower Damodar Basin. This is important, because availability of accurate bank or

20   embankment heights can be a decisive factor for maintaining model stability at extreme flow conditions

21   in 1D hydrodynamic models, as this information is crucial for containing the water within the channel. A

22   ground survey along the longitudinal profile of the study reach was also essential for employing

23   LISFLOOD-FP because the channel bed elevation derived from the SRTM DEM would have yielded an

24   inaccurate energy gradient for the river. In particular, the presence of high frequency noise in the channel

25   portion of the SRTM DEM (Fig. 8a) would interrupt the monotonic slope of the LISFLOOD-FP channel

1   vector. The simple formulation and data requirement of the LISFLOOD-FP model enabled us to take full

2   advantage of limited ground surveys to overcome the shortcomings of the SRTM DEM.

3

4   *6.2.   Flood routing model*

5

6   The high performance of LISFLOOD-FP with very low values of Manning's n is consistent with the

7   wide, deep channel in the study area. The average channel width of the study reach is ~1 km and average

8   bankfull depth is more than 12 m, meaning that channel roughness has very limited influence over the

9   flow pattern as only a small fraction of the flowing water is subjected to frictional drag of the channel bed

10 and banks. The model consistently underestimated the rising limb of the observed stage hydrograph and

11 shows some degree of error, particularly in the validation case, in simulating the receding level of flood

12 water. Underestimation of the modelled stage hydrograph is not a serious concern because the 20 to 21 m

13 river stage is well below the bankfull level at Jamalpur (cross-section 7 in Fig. 6). The error in river stage

14 (0.5 to 1 m at the peak) is not more than 5 percent of the bankfull channel depth of approximately 24 m at

15 Jamalpur. Slight underestimation of the rising limb may be explained by the fact that we have not

16 considered the amount of rainfall received directly by the reach and its immediate surrounding that is

17 directly fed into the channel of the Damodar River. Overestimation of the falling limb of a flood

18 hydrograph is also expected as the terrain data are not sufficiently accurate to represent smaller conduits

19 and depressions through which the floodwater escapes after the peak flow. Slight underestimation of the

20 supply of water in the channel also explains the slight delay in the simulated flood peak, because

21 additional water would have increased the flood wave velocity by reducing the influence of frictional

22 drag. Finally, we were able to obtain reasonable results despite not incorporating the inline structure and

23 two bridges that occur in the study reach. These structures thus appear to have had a very limited

24 influence in altering the flow pattern, probably due to the extreme nature of the modelled flow regimes. In

1 this respect, the finding of this paper is encouraging for developing countries, as limited but reasonably

2 accurate data appear to be sufficient for routing extreme floods using freely available and computationally

3 less demanding models. However, such coarse inputs and simple models may not be appropriate for

4 routing the normal or low flows of a river.

5

6   *6.3.   Uncertainty analysis*

7 Although the overall trend in the performance of the model for the MonteCarlo runs (Fig 16a) broadly

8 followed the sensitivity graph of the channel n values (Fig 12), the wide range of variation in the

9 performance measure for each channel n value is probably due to the influence of DEM uncertainty,

10 especially in terms of bank heights that determine the exchange of water between the 1D channel

11 component and the 2D floodplain component. The variation in model performance for different stages at

12 the downstream boundary and channel width values was probably a result of variations in other factors,

13 particularly the channel friction and input DEMs.

14 Unlike Hunter et al. (2005) we have not used multiple channel roughness coefficients for different sub-

15 reaches, as we did not have observed stage records at any intermediate points to evaluate the sensitivity of

16 n for a specific sub-reach. The narrow range of the uncertainty lines in Fig. 17 is also encouraging for our

17 confidence in the modelled output. As mentioned in Section 3 the difference in the vertical datum of the

18 SOI and the EGM96 geoid based measurements leads to a certain degree of mismatch in elevation values

19 which varies from place to place. The Jamalpur gauging station uses the SOI elevation while our model

20 used the WGS84 and EGM96 to derive the orthometric heights which were used as an equivalent of the

21 elevation from the mean sea level (MSL). This uncertainty in the measurements of river stages is

22 represented by the $\pm$ 20 cm error bars in Fig. 17. The approximate error limit was derived by comparing

23 the GPS-EGM96 heights at 2 points with known SOI elevations near Jamalpur. The SOI vertical datum is

24 derived from a network of tidal gauges and there is no satisfactory geoid model available for India to

25 accurately derive the orthometric heights from GPS (Agrawal 2005). In contrast, most freely available

24

geospatial data such as the SRTM DEM use a global datum. Mismatch of local and global datum is quite common and the absence of robust local geoid models in many developing countries poses a challenge for using global data in applications like flood modelling where sub-metre accuracy is essential.

7.0. Conclusion

The intention of this study is to explore a low-cost methodology for predicting the dynamics of hazardous flood events. We found that a simple model (LISFLOOD-FP) combined with relatively coarse terrain and hydrologic inputs can perform this task with reasonable accuracy, with an index of agreement d of 0.77 with observed river stage time series. We have demonstrated that limited but well-designed field surveys can supplement freely-available moderate resolution DEMs for the purpose of hydraulic routing of extreme floods. We have also pointed out typical obstacles that are encountered in the developing world for hydrodynamic modelling such as the dearth of accurate terrain data, shortage of river gauging stations, absence of permanent GPS base station data in the public domain, and the lack of well-defined local geoid models, and suggested some techniques to overcome them. The limitations arising from the use of coarse hydrologic and terrain inputs may not be very significant when we are interested in routing bankfull discharge but can be quite critical for modelling normal to low flow. Our study also provides an alternative to purely cross-section based 1D hydraulic routing of floods, particularly for river reaches where the quality of the SRTM DEM is not good enough to extract accurate cross-sections. The assessment of uncertainty that arose due to the use of sparse inputs illustrated that a significant portion of the observed records were within a narrow range of uncertainty bounds and boosts our confidence that the current setup can be employed in flood management practice in developing countries.

1   Acknowledgement

References

Agrawal NK (2005) Geodetic infrastructure in India, Coordinates 1(7). http://mycoordinates.org/geodetic-infrastructure-in-india/ Accessed online on 30th January, 2012

Alcántara-Ayala I (2002) Geomorphology, natural hazards, vulnerability and prevention of natural disasters in developing countries. Geomorphology 47:107-124.

Aronica G, Bates PD, Horritt M S (2002) Assessing the uncertainty in distributed model predictions using observed binary pattern information within GLUE. Hydrological Processes 16: 2001–2016.

Bates PD, DeRoo APJ (2000) A simple raster-based model for flood inundation simulation. Journal of Hydrology 236:54-77.

Bates PD, Wilson MD, Horritt MS, Mason D, Holden N, Currie A (2006) Reach scale floodplain inundation dynamics observed using airborne synthetic aperture radar imagery: Data analysis and modelling. Journal of Hydrology 328:306–318.

Bates PD, Horritt MS, Fewtrell TJ (2010) A simple inertial formulation of the shallow water equations for efficient two-dimensional flood inundation modelling. Journal of Hydrology 387:33-45.

Beven KJ and Binley AM (1992) The future of distributed models: model calibration and uncertainty prediction Hydrological Processes 6:279–298.

Beven KJ (2001) Rainfall-runoff modelling-The primer. John Wiley and Sons, Chichester, p-235.

Beven K (2010) Environmental modelling: An uncertain future? An introduction to techniques for uncertainty estimation in environmental prediction. Routledge, pp 121

Casas A, Benito G, Thorndycraft V, Rico M (2006) The topographic data source of digital terrain models as a key element in the accuracy of hydraulic flood modelling. Earth Surf. Process. Landforms 31: 444–456.

Central Technical Power Board, Preliminary memorandum on the development of the Damodar River, (1948) Government of India Press, Kolkata.

Chandra S (2003) India: Flood management-Damodar River Basin, World Meteorological Organization. www.apfm.info/pdf/case_studies/cs_india.pdf. Accessed 29th March 2012

Chow VT (1959) Open channel hydraulics. McGraw-Hill, New York.

Ebner R, Featherstone WE (2008) How well can online GPS PPP post-processing services be used to establish geodetic survey control networks. J of Applied Geodesy 2:149-157.

El-Mowafy A (2011) Analysis of web-based GNSS post-processing services for static and kinematic positioning using short data spans. Survey Review 43:535-549.

Farr TG, Rosen PA, Caro E, Crippen R, Duren R, Hensley S, Kobrick M, Paller M, Rodriguez E, Roth L, Seal D, Shaffer S, Shimada J, Umland J, Werner M, Oskin M, Burbank, D, Alsdorf D (2007) The shuttle radar topography mission. Reviews of geophysics 45, RG2004, 1-33.

Gorokhovich Y, Voustianiouk A (2006) Accuracy assessment of the processed SRTM-based elevation data by CGIAR using field data from USA and Thailand and its relation to the terrain characteristics. Remote Sensing of Environment 104:409-415.

Garbrecht J, Brunner G. (1991) Hydrologic Channel-Flow Routing for Compound Sections. J. Hydraul. Eng., 117(5), 629–642. doi: 10.1061/(ASCE)0733-9429(1991)117:5(629)

Hall JW, Tarantola S, Bates PD, Horritt, MS (2005) Distributed Sensitivity Analysis of Flood Inundation Model Calibration. Journal of Hydraulic Engineering 131:117-126.

Hofton M, Dubayah R, Blair JB, Rabine D (2006) Validation of SRTM elevations over vegetated and non-vegetated terrain using medium flootprint lidar. Photogrammetric Engineering and Remote Sensing 72:279-285.

Horritt MS and Bates PD (2001) Predicting floodplain inundation: raster-based modelling versus the finite-element approach. Hydrological Processes 15: 825–842.

Horritt MS and Bates PD (2001) Evaluation of 1D and 2D numerical models for predicting river flood inundation Journal of Hydrology 268:87-99.

Hunter NM, Bates PD, Horritt MS, De Roo APJ, Werner MGF (2005) Utility of different data types for calibrating flood inundation models within a GLUE framework. Hydrology and Earth System Sciences 9:412-430.

Jarvis A, Reuter HI, Nelson A, Guevara E (2008) Hole-filled SRTM for the globe Version 4, available from the CGIAR-CSI SRTM 90m Database (http://srtm.csi.cgiar.org).

Legates DR and McCabe Jr GJ (1999) Evaluating the use of "goodness-of-fit" measures in hydrologic and hydroclimatic model validation. Water Resour Res 35: 233–241.

Lemoine FG, Smith DE, Kunz L, Smith R, Pavlis EC, Pavlis NK, Klosko SM, Chinn DS, Torrence MH, Williamson RG, Cox CM, Rachlin KE, Wang YM (1996) The development of the NASA GSFC and NIMA joint geopotential model. Proceedings for the International Symposium on Gravity, Gravity, Geoid, and Marine Geodesy, (GRAGEOMAR 1996), The University of Tokyo, Tokyo, Japan, September 30 to October 5, 1996.

Mason DC, Schumann G, Bates PD (2010) Data Utilization in Flood Inundation Modelling, in Flood Risk Science and Management (eds G. Pender and H. Faulkner), Wiley-Blackwell, Oxford, UK. doi: 10.1002/9781444324846.ch11

Neal J, Schumann G, Fewtrell T, Budimir M, Bates P, Mason D (2011) Evaluating a new LISFLOOD-FP formulation with data from the summer 2007 floods in Tewkesbury, UK. Journal of Flood Risk Management, 4: 88–95.

Paiva RCD, Collischonn W, Tucci CEM (2011) Large scale hydrologic and hydrodynamic modeling using limited data and a GIS based approach. Journal of Hydrology 406:170-181.

Pappenberger F, Matgen P, Beven, KJ, Henry J-B, Pfister L, Fraipont de P (2006) Influence of uncertain boundary conditions and model structure on flood inundation predictions. Advances in Water Resources, 29: 1430-1449.

Patro S, Chatterjee C, Singh R, Raghuwanshi NS (2009a) Hydrodynamic modelling of a large flood-prone river system in India with limited data. Hydrological Processes 23:2774-2791.

Patro S, Chatterjee C, Singh R, Raghuwanshi NS (2009b) Flood inundation modeling using MIKE FLOOD and remote sensing data. J Indian Soc Remote Sens 37:107-118.

Petersen G, Fohrer N (2010) Two-dimensional numerical assessment of the hydrodynamics of the Nile swamps in southern Sudan. Hydrol. Sci. J. 55:17–26.

Pramanik N, Panda RK, Sen D (2010) One dimensional hydrodynamic modelling of river flow using DEM extracted river cross-sections. Water Resour Manage 24:835-852.

Reuter H, Nelson A, Strobl P, Mehl W, Jarvis A (2009) A first assessment of Aster GDEM tiles for absolute accuracy, relative accuracy and terrain parameters. Proceedings of the Geoscience and Remote Sensing Symposium,IGARSS 2009 IEEE International. pp. 240-243.

Saha SK (1979) River-Basin planning in the Damodar Valley of India. Geographical Review 69:273-287.

Sanders R, Shaw F, Mackay H, Galy H, Foote M (2005) National flood modeling for insurance purposes: using IFSAR for flood risk estimation in Europe. Hydrology and Earth System Sciences 9: 449-456.

Sanders BF (2007) Evaluation of on-line DEMs for flood inundation modeling. Advances in Water Resources 30:1831-1843.

Sanyal J, Lu XX (2004) Application of remote sensing in flood management with special reference to monsoon Asia: a review. Natural Hazards 33:283–301.

Slater JA, Garvey G, Johnston C, Haase J, Heady B, Kroenung G, Little J (2006) The SRTM data "finishing" process and products. Photogrammetric Engineering and Remote Sensing, 72(0), 237-247.

Stephens EM, Bates PD, Freer J, Mason D (2012) Calibration of flood inundation models using uncertain satellite observed water levels. Journal of Hydrology.

DOI: http://dx.doi.org/10.1016/j.jhydrol.2011.10.040

Trigg MA, Wilson MD, Bates PD, Horritt MS, Alsdorf DE, Forsberg BR, Vega MC (2009) Amazon flood wave hydraulics. Journal of Hydrology, 374(1-2), 92-105.

Tsakiri M (2008) GPS processing using online services. J of Surveying Eng 134:115-125.

Willmot CJ (1984) On the evaluation of model performance in physical geography. In: Gaile GL, Willmot CJ, Reidel D (ed) Spatial Statistics and Models, Dordrecht, pp 443–460.

Wilson M, Bates P, Alsdorf D, Forsberg B, Horritt M, Melack J, Frappart F, Famiglietti J (2007) Modeling large-scale inundation of Amazonian seasonally flooded wetlands. Geophysical Research Letters 34:L15404.

Wilson MD (2012) readstage.m (available under GNU General Public Licence) http://www.mdwilson.org/research-background/useful-code Accessed 30th January 2012
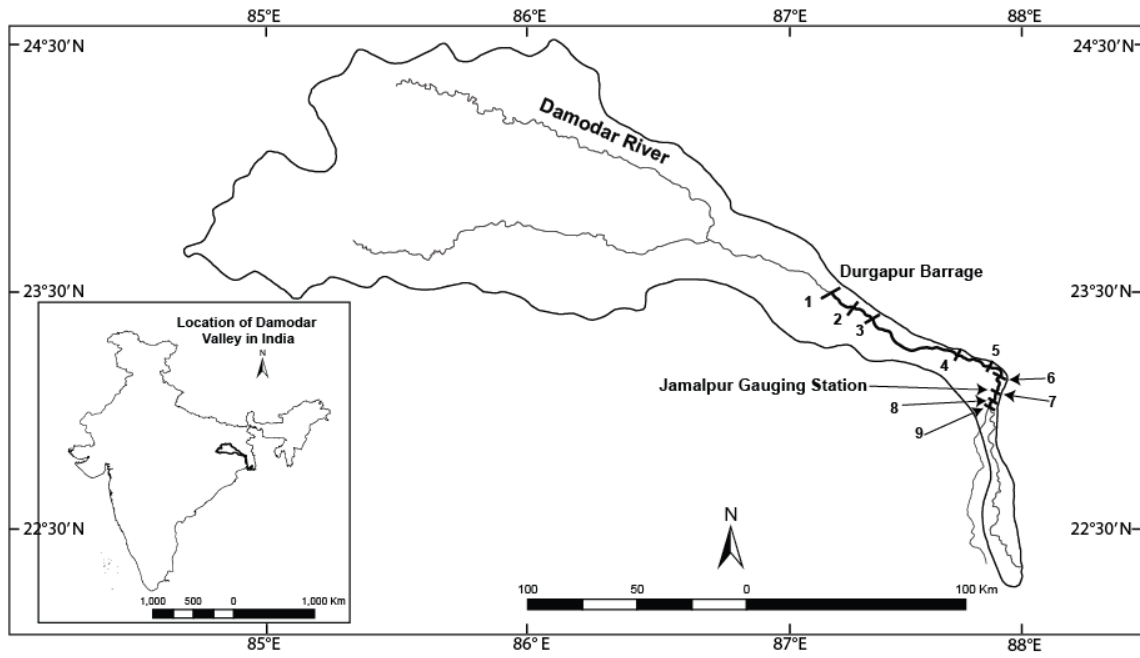
Fig. 1 Overview of the Damodar Basin. The study reach is shown by heavy lines, and the surveyed cross-sections are indicated by numbers.
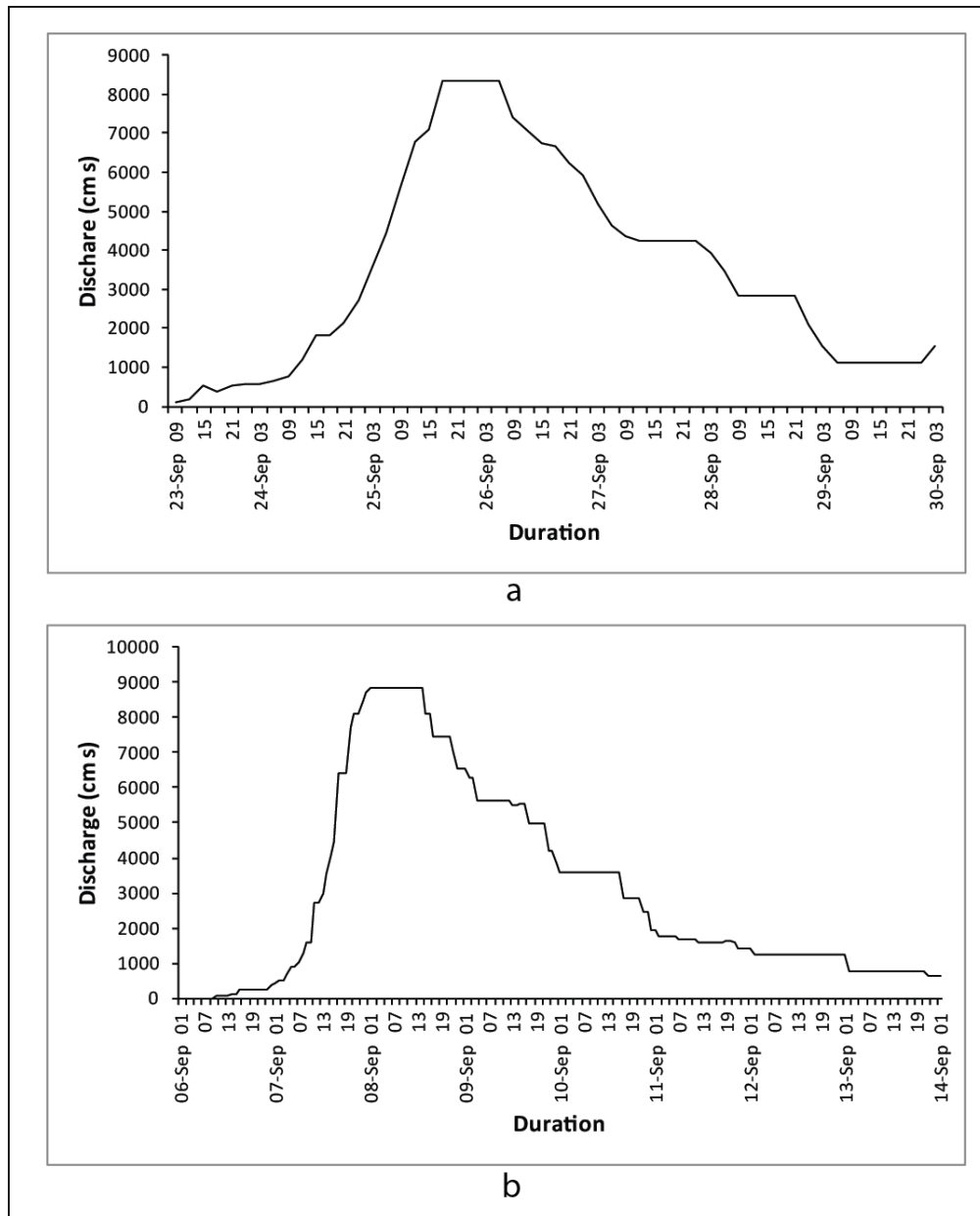
Fig. 2 Hydrographs at Durgapur Barrage of the 2007 (a) and 2009 (b) flood events. Data were obtained at 3 hour and 1 hour intervals for the 2007 and 2009 events respectively.
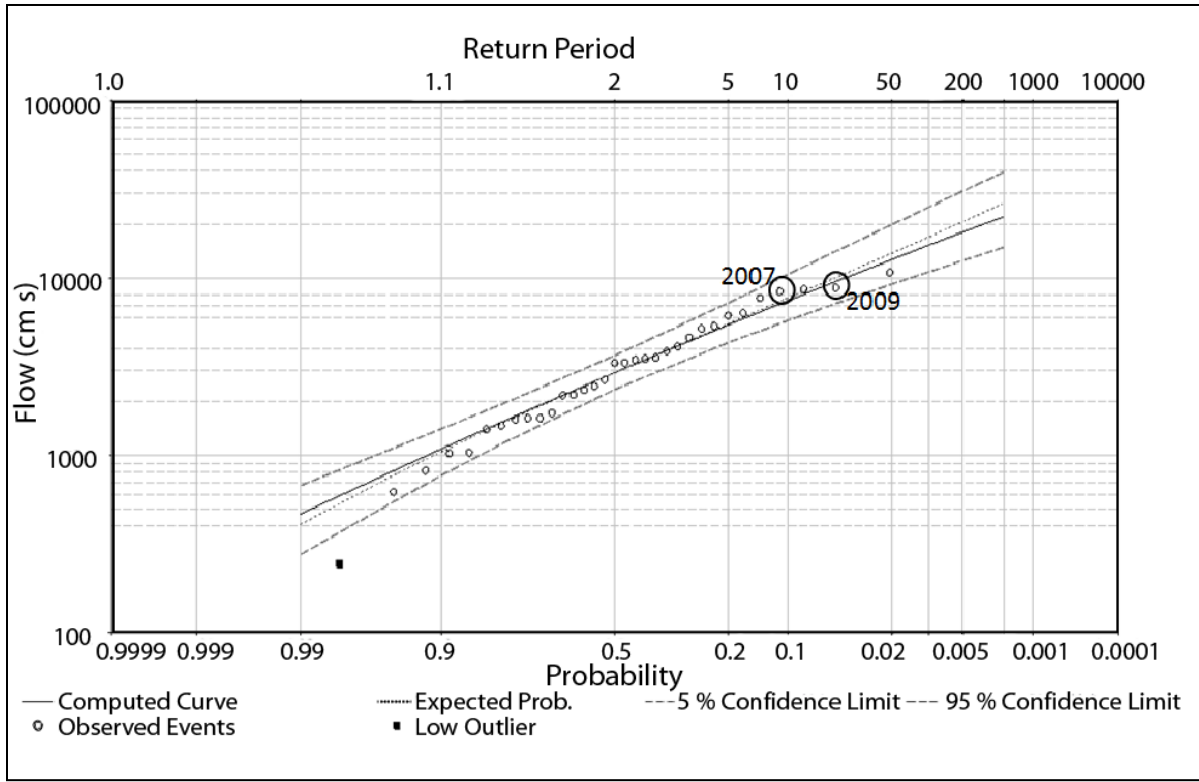
Fig. 3 Flood frequency analysis of the annual peak discharge from the Durgapur Barrage. The 2007 and 2009 events, which are highlighted with circles, were used for calibration and validation respectively.
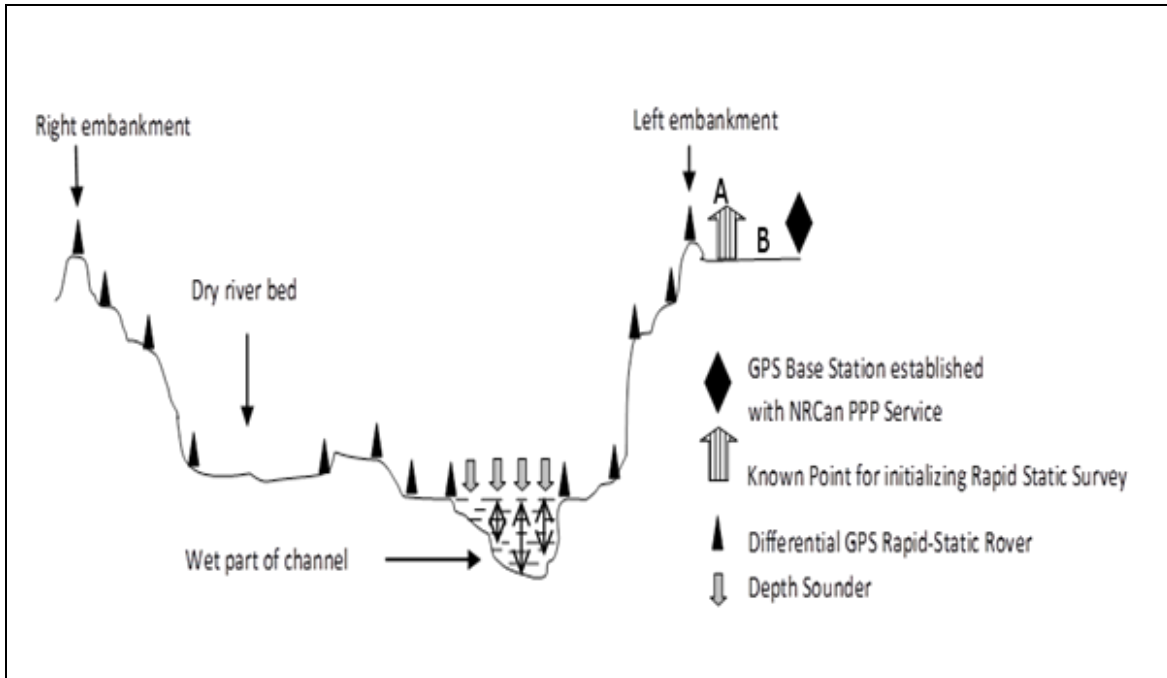
Fig. 4 Schematic diagram illustrating the cross-section survey geometryalong the Damodar River with differential GPS and depth sounder. NRCan PPP is the abbreviated form of Natural Resources Canada Precise Point Positioning.
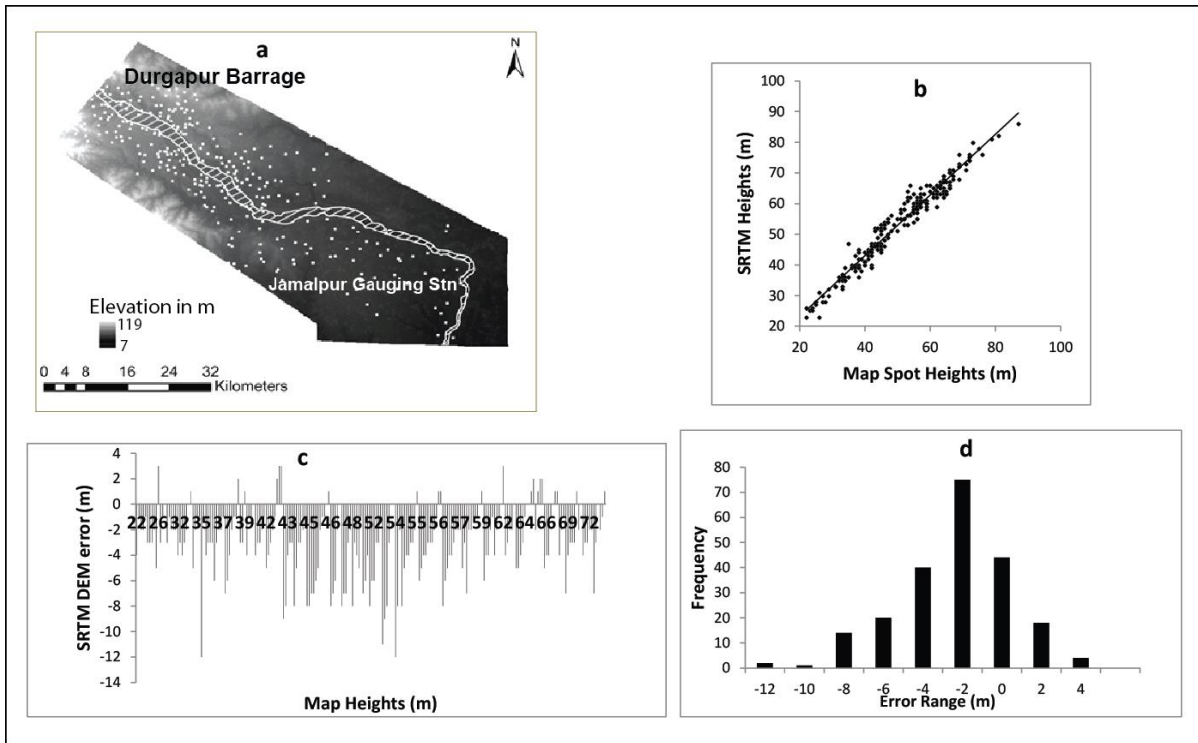
Fig. 5 Distribution of error in the SRTM DEM. a, location of the Survey of India spot heights for computing the SRTM DEM errors. b, scatter plot of the SRTM DEM and Survey of India spot heights. c, occurrence of error, calculated as the difference between the SRTM DEM and the spot heights, in different elevation ranges (negative values signify that SRTM DEM is higher than SOI spot heights). d, Histogram of the errors in showing their distribution; 28.4 % of the points are within 2 m of error.
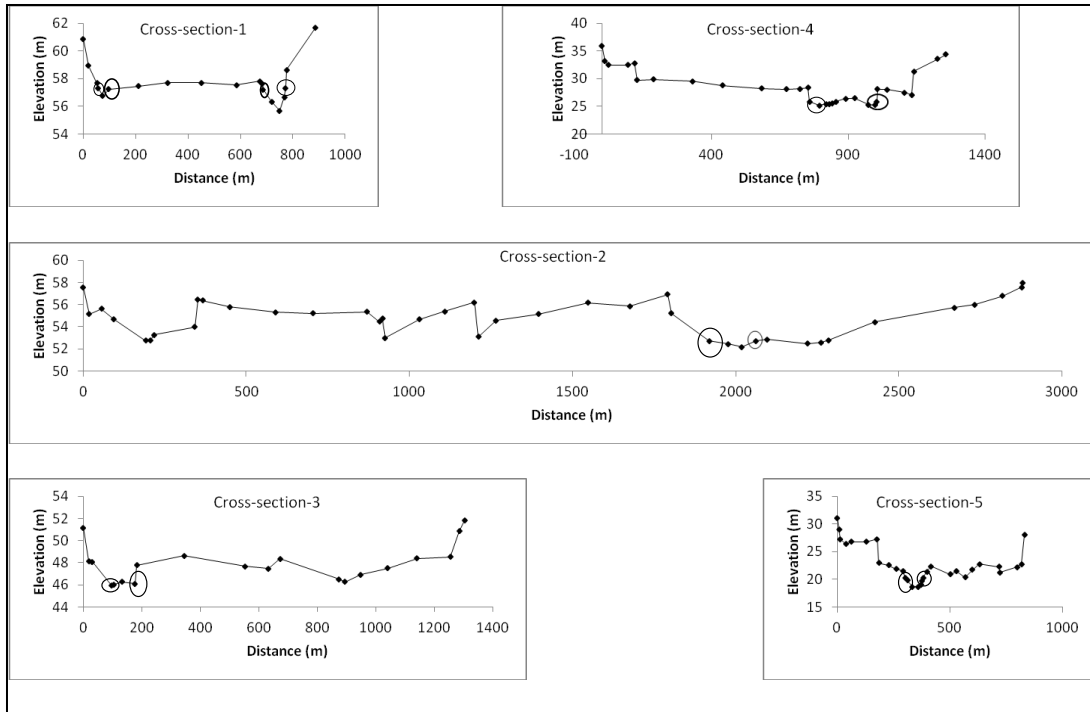
Fig. 6 Surveyed cross-sections (1-5). See Fig. 1 for locations. Surveyed points that are marked with circles show the water level during the survey.
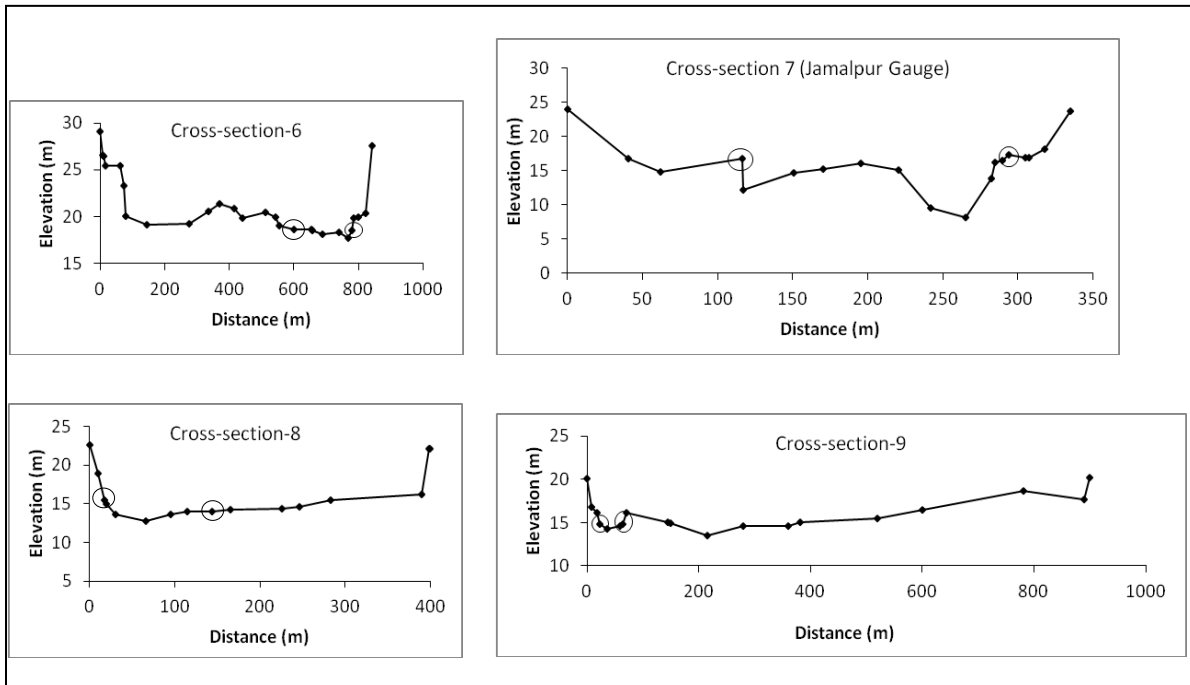
Fig. 7 Surveyed cross-sections (6-9). Surveyed points that are marked with circles show the water level during the survey. A smaller horizontal scale was used for cross-sections 7 and 8 to properly depict the configuration of the channel in these two locations, where the channel is narrow and deep.
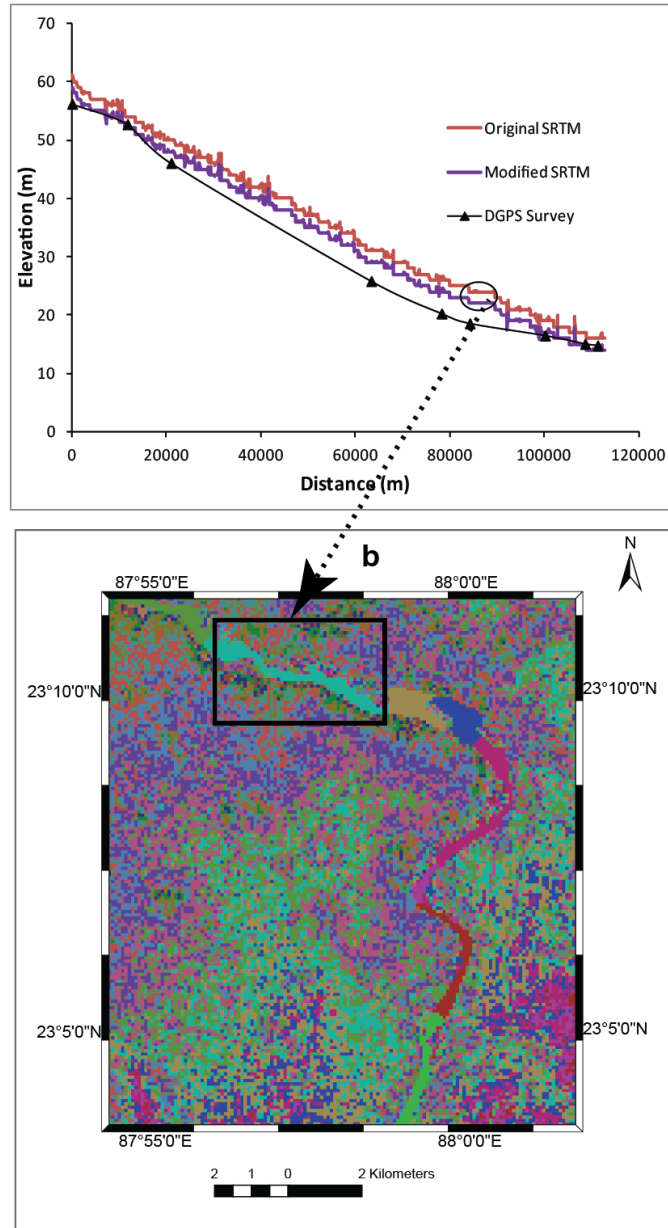
Fig. 8 Long profile of the study reach. a, comparison between the profiles derived from the original SRTM DEM, modified DEM and field survey. The slopes of the surveyed profile at the extreme upstream and downstream of the study reach are distinctly different from those derived from the SRTM DEM or its modified form . b, example of the extensive flat surface in the channel portion of the original SRTM DEM. Unique elevation values are represented in unique colours to show homogeneous values over the channel, depicting spurious flat surfaces.

Fig. 9 Representation of an island in the Damodar River within LISFLOOD-FP. Red arrows show the 1D configuration of the main channel. The shallower secondary channel and the floodplain, depicted with shading, are handled by the 2D component of the model.
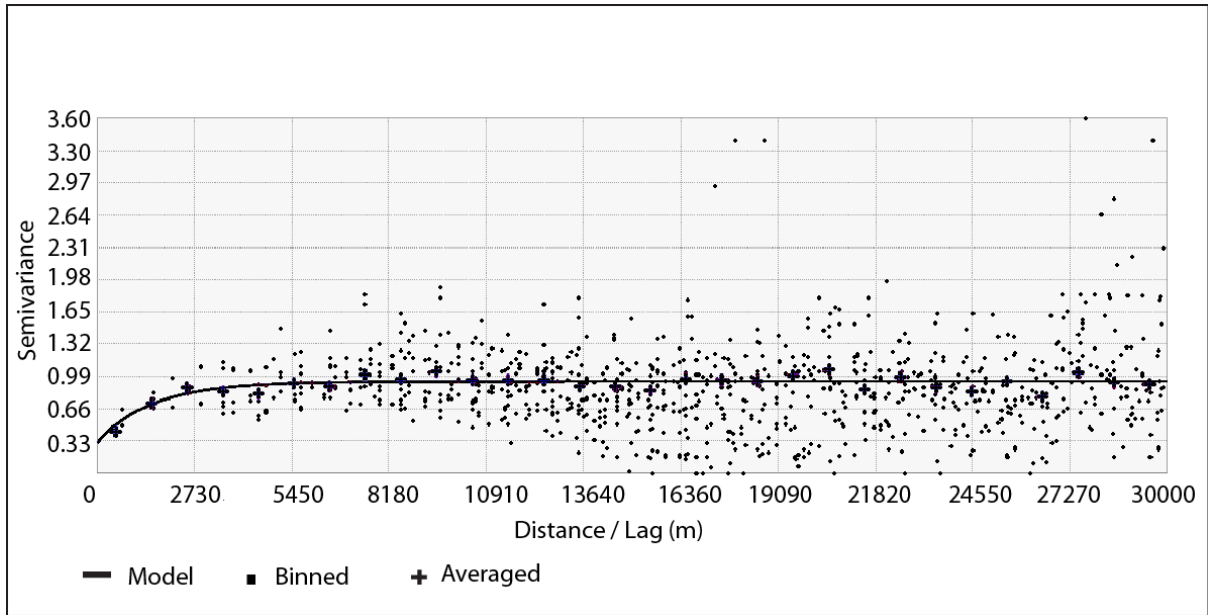
Fig 10 Semivariogram model derived from the error of the modified SRTM DEM measured at the location of available spot heights from Survey of India topographic maps.
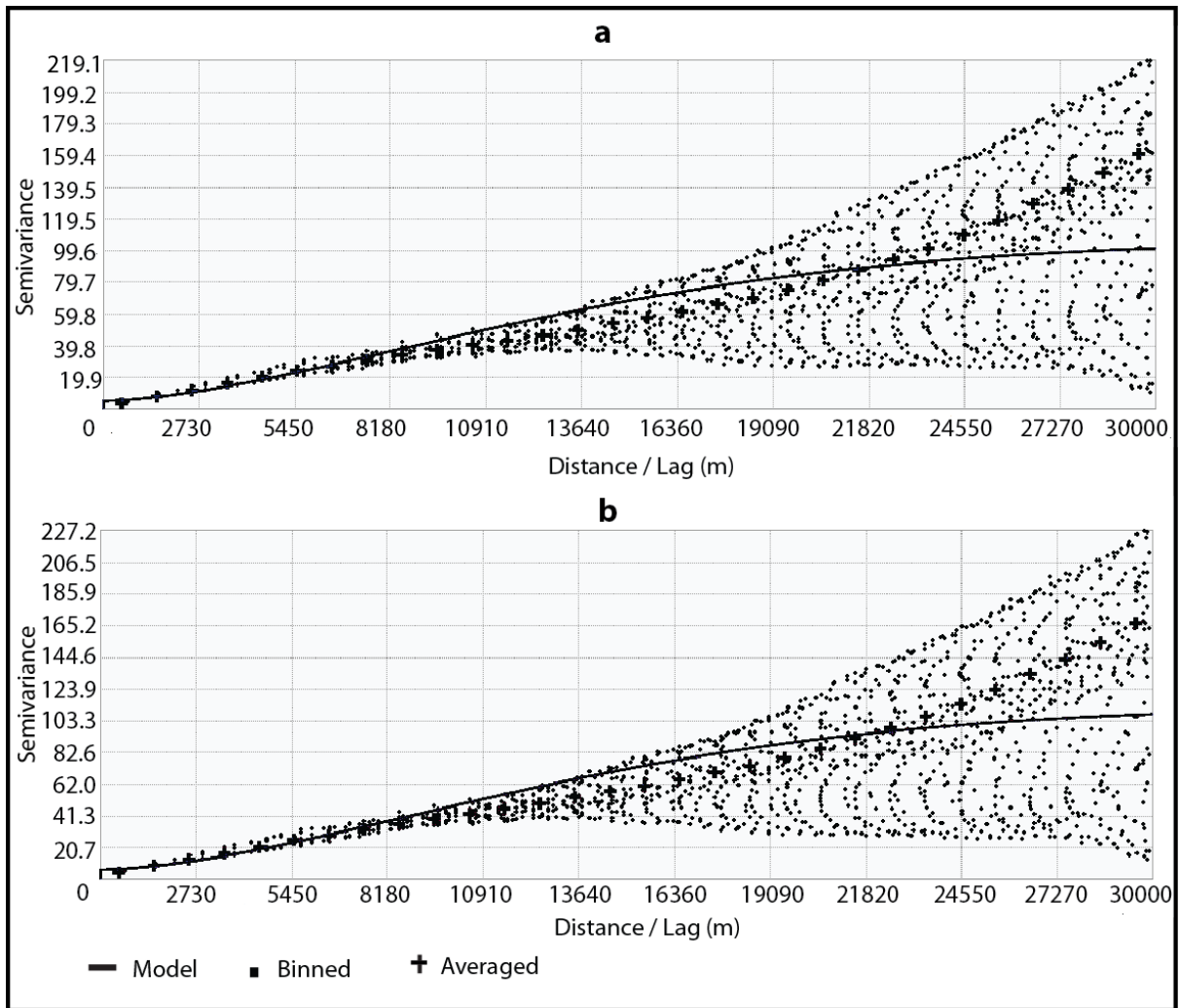
Fig 11 Semivariograms of the input DEMs for LISFLOOD-FP model. a, semivariogram of the modified SRTM DEM. b, semivariogram of a DEM where the error surface derived from Gaussian Sequential Simulation was added with the modified SRTM data.
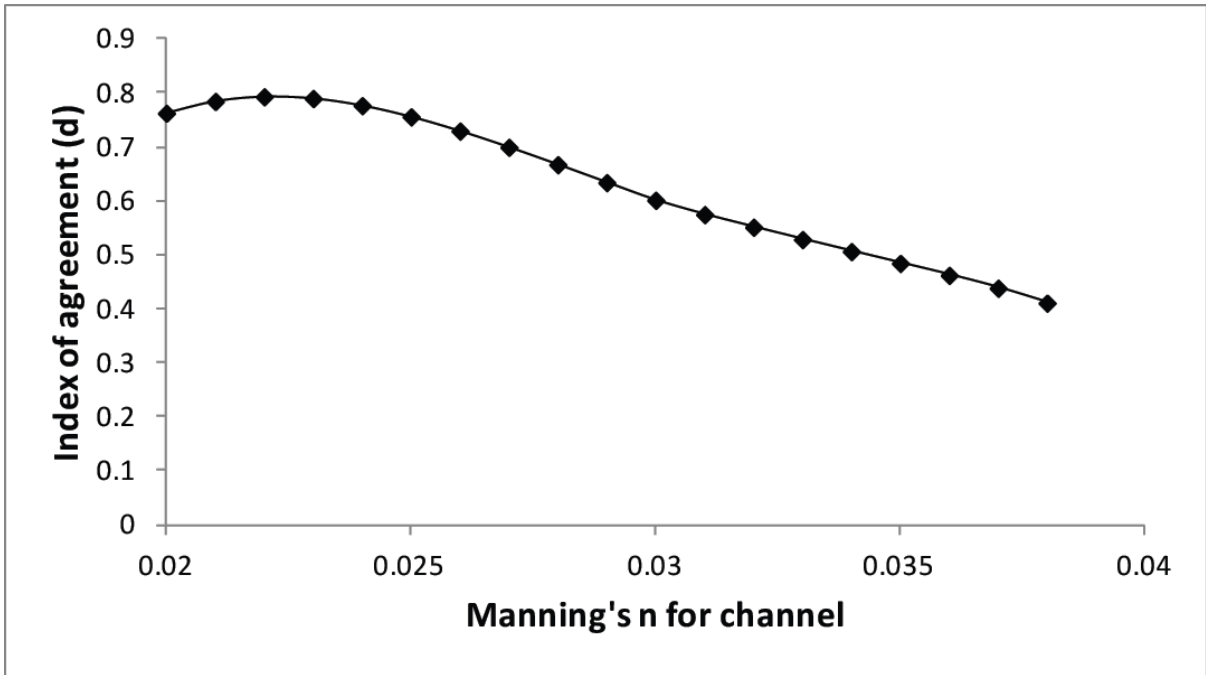
Fig 12 Performance of LISFLOOD-FP with different channel roughness coefficients during calibration with the 2007 flood event. The performance of the model peaked at a channel Manning's n of 0.022 but declined with further reduction in roughness.
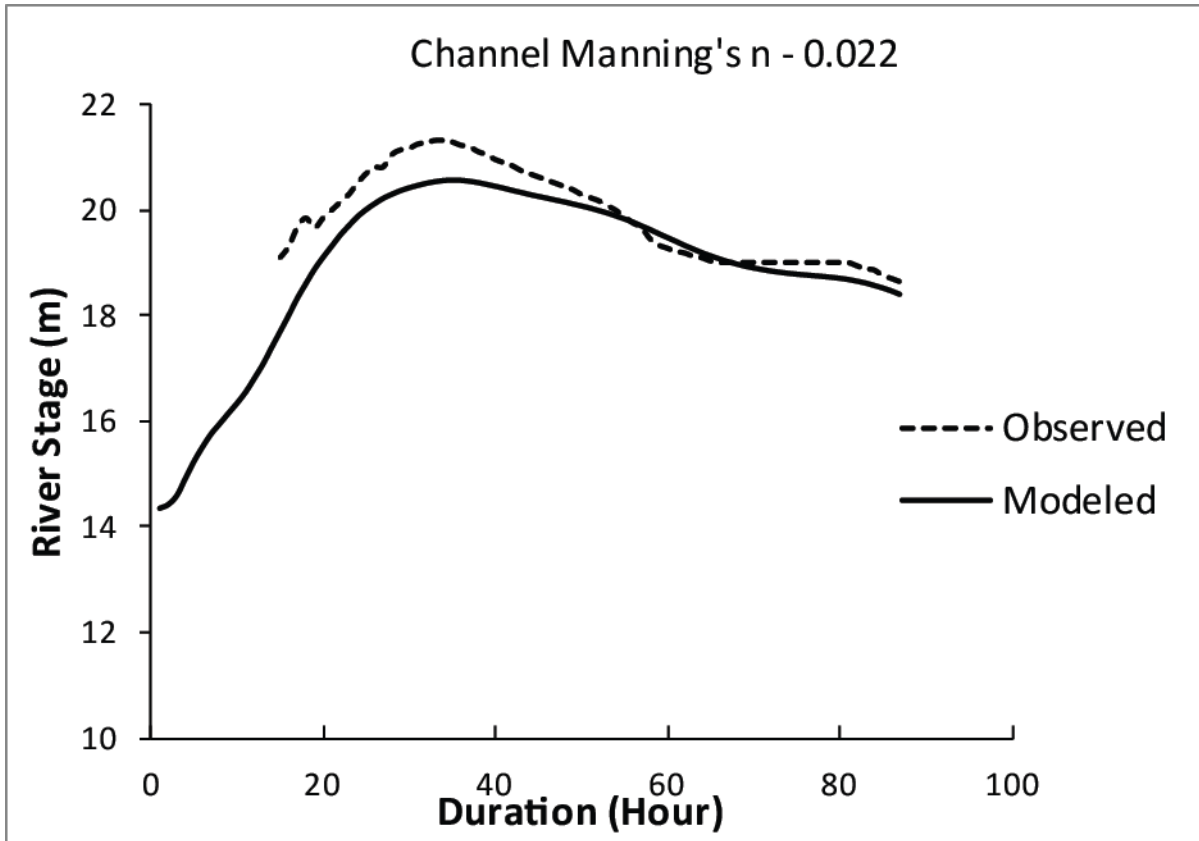
Fig. 13 Best calibrated output of modelled stages from LISFLOOD-FP at Jamalpur gauging station for a global channel Manning's n of 0.022.
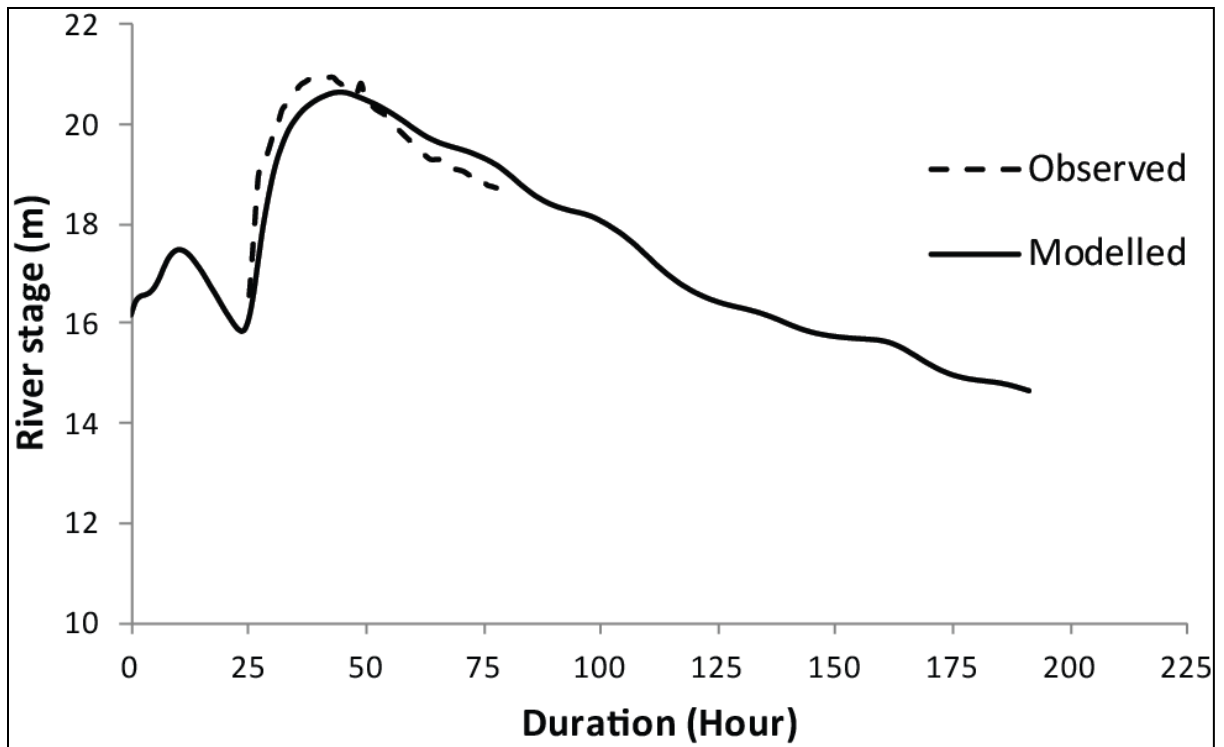
Fig 14 Validation of the LISFLOOD-FP model using the modelled and observed stage data at Jamalpur gauging station for the 2009 extreme flood event. The calibrated value of n as 0.022 was used for the channel.
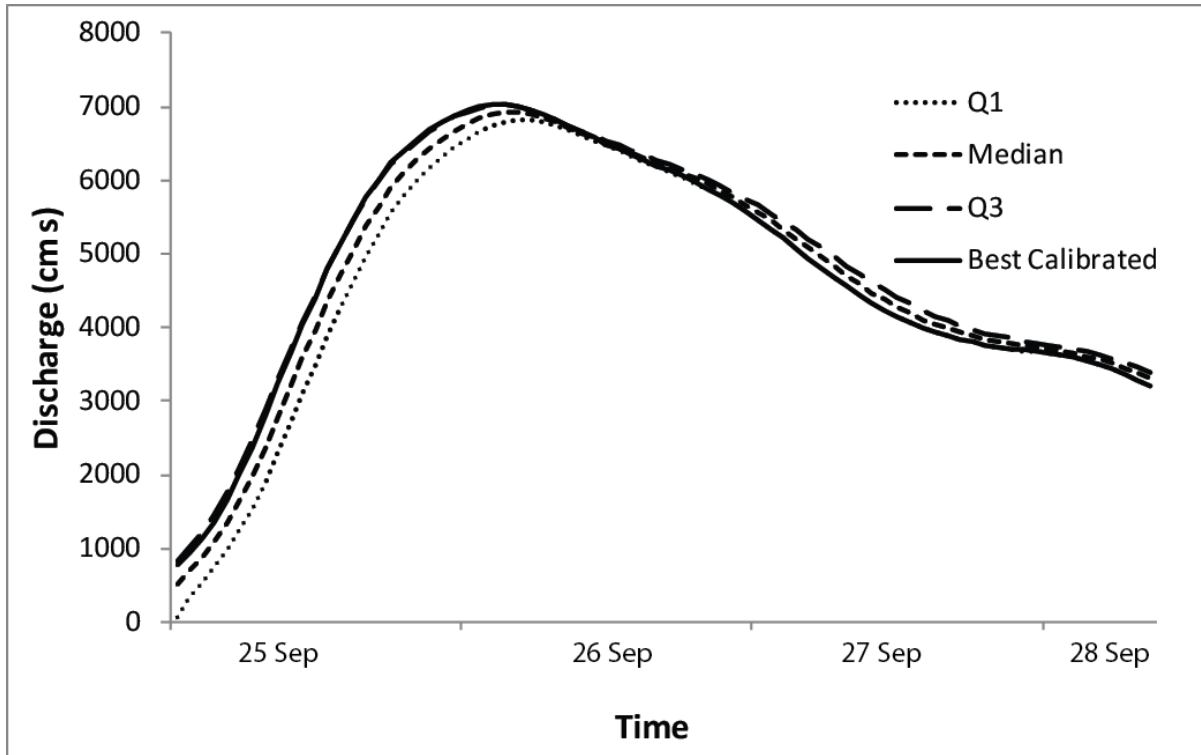
Fig15 Variability of the predicted discharge hydrograph at the model downstream boundary for 3000 MonteCarlo simulation. Variability of the modelled figures at each time step is shown by 1st quartile, median and 3rd quartile figures of 3000 results. The modelled output from the best calibrated case is presented as a benchmark of accuracy.
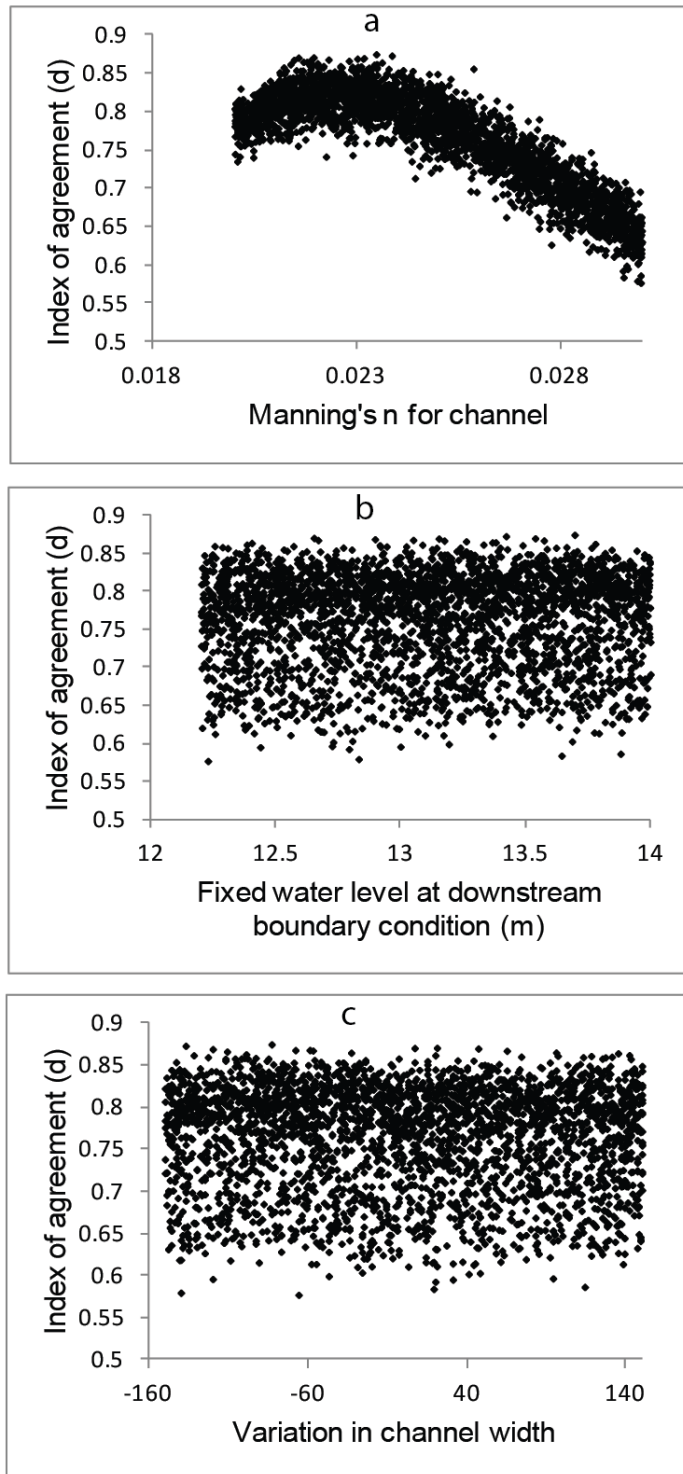
Fig 16 Dotty plots showing the sensitivity of the model to variations in (a) the channel roughness coefficient, (b) the imposed arbitrary water level at the downstream boundary for the 2007 flood event and (c) channel width at a particular point in the channel vector.
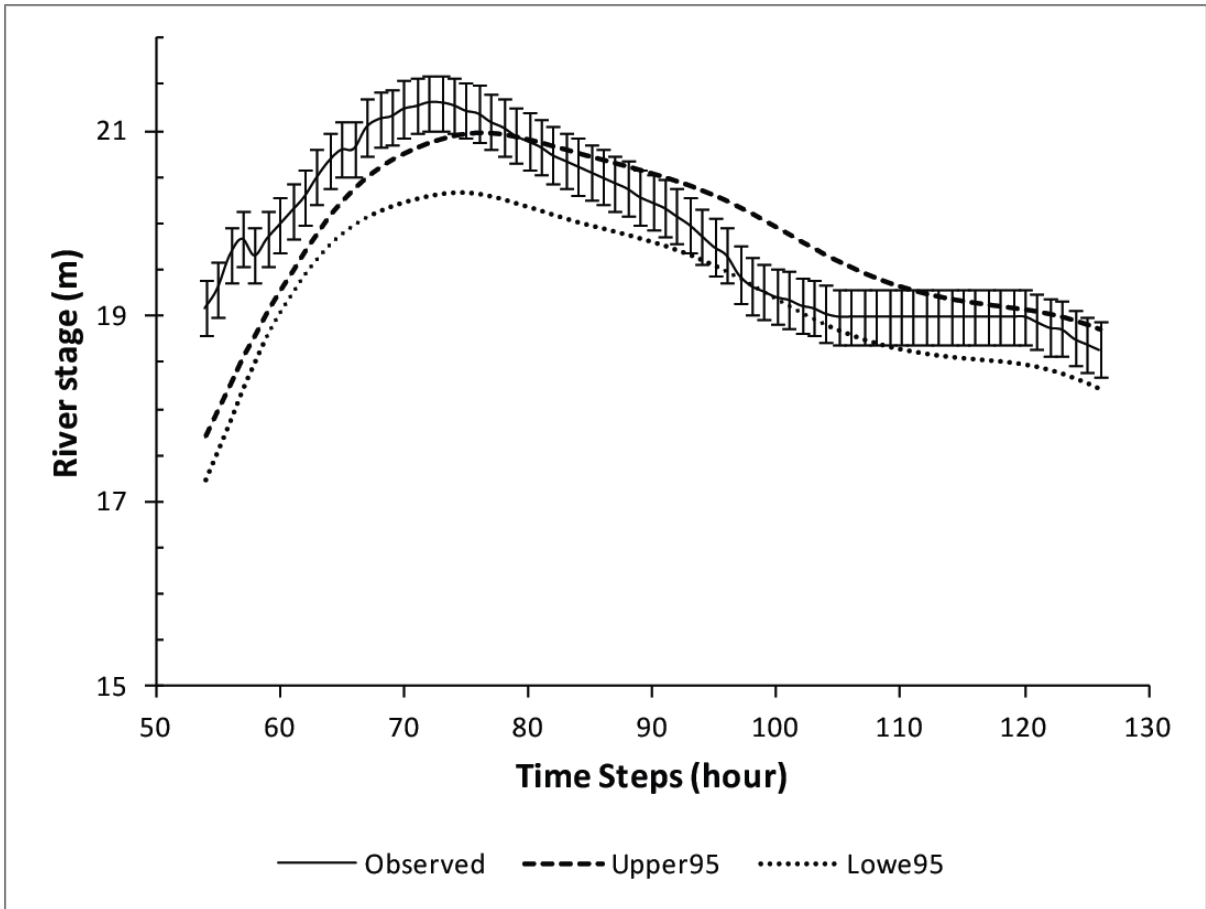
Fig 17 Uncertainty plot of the LISFLOOD-FP model of the 2007 flood event showing 95 percent upper and lower uncertainty bounds. Uncertainty in the observed river stages is shown by a ± 20 cm vertical error bar.